Published in final edited form as:
Neuroscience. 2010 December 1; 171(2): 566–576. doi:10.1016/j.neuroscience.2010.08.058.

Derangements of Post-ischemic Cerebral Blood Flow by Protein Kinase C Delta

Hung Wen Lin, **R. Anthony DeFazio**, **David DellaMorte**, **John W. Thompson**, **Srinivasan V. Narayanan**, **Ami P. Raval**, **Isabel Saul**, **Kunjan R. Dave**, and **Miguel A. Perez-Pinzon**
Cerebral Vascular Disease Research Center, Department of Neurology, University of Miami, Miller School of Medicine, Miami, FL 33136.

Abstract

Cerebral ischemia causes blood flow derangements characterized by hyperemia (increased cerebral blood flow, CBF) and subsequent hypoperfusion (decreased CBF). We previously demonstrated that protein kinase C delta (δPKC) plays an important role in hippocampal neuronal death after ischemia. However, whether part of this protection is due to the role of δPKC on CBF following cerebral ischemia remains poorly understood. We hypothesized that δPKC exacerbates hyperemia and subsequent hypoperfusion resulting in CBF derangements following ischemia. Sprague-Dawley (SD) rats pretreated with a δPKC specific inhibitor (δV1-1, 0.5 mg/kg) exhibited attenuation of hyperemia and latent hypoperfusion characterized by vasoconstriction followed by vasodilation of microvessels after 2-vessel occlusion plus hypotension measured by 2-photon microscopy. In an asphyxial cardiac arrest model (ACA), SD rats treated with δV1-1 (pre- and post-ischemia) exhibited improved perfusion after 24 hrs and less hippocampal CA1 neuronal death 7 days after ACA. These results suggest possible therapeutic potential of δPKC in modulating CBF and neuronal damage after cerebral ischemia.

Keywords

Protein Kinase C Delta; Asphyxial Cardiac Arrest; Neuroprotection; Two-vessel Occlusion; Two-photon Microscopy; Cerebral Ischemia

Cerebral ischemia is defined by little or no-blood flow in cerebral circulation characterized by low oxygen, glucose, and accumulation of metabolic products (Hossmann, 1997). A form of global cerebral ischemia (i.e. cardiac arrest), which affects whole-brain vascular dynamics, promotes neuronal cell death in many brain regions including the hippocampus (Raval et al., 2005; Dave et al., 2006). It is well accepted that reperfusion after cerebral ischemia may substantially cause increased injury characterized by two phases: rapid hyperemia (increased blood flow) and delayed hypoperfusion (decreased blood flow) (Watson and Ginsberg, 1989; Choi, 1993). These derangements of cerebral blood flow (CBF) have been implicated in injury after global cerebral ischemia (Hosomi et al., 2007). Upon reperfusion, hyperemia and

Corresponding author: Miguel A. Perez-Pinzon, Ph.D., Department of Neurology, D4-5, University of Miami Miller School of Medicine, P.O. Box 016960, Miami, FL 33101, Phone: (305) 243-7698, Fax: (305) 243-5830, perezpinzon@miami.edu.

Disclosure/Conflict of Interest: The authors have no conflict of interest in this manuscript.

subsequent hypoperfusion of cerebral blood vessels (Hossmann, 1997) leads to enhanced superoxide generation (Koller et al., 2004; Zhao et al., 2006). The hyperemia phase leads to ischemia-induced cell death to different areas of the brain (Zhao et al., 2006) as well as decreased blood flow (hypoperfusion) (Caplan et al., 2006) resulting in yet another possible ischemic/hypoxic condition.

Several lines of evidence suggest that a protein kinase C (PKC) isozyme, namely δPKC, plays an important role in mediating cerebral reperfusion injury after ischemia (Bright et al., 2004). More specifically, δPKC has been implicated in hallmarks of post-ischemic injury including oxidative stress, apoptosis, and inflammation (Brodie and Blumberg, 2003). Previously, we demonstrated activation of a similar pathway played a key role in CA1 rat hippocampal histopathology following asphyxial cardiac arrest (ACA) (Raval et al., 2005). Thus, we cannot rule out that the neuroprotection afforded by the δPKC inhibitor in our previous study after ACA (Raval et al., 2005) was due to CBF modulation.

δPKC modulates micro-cerebrovascular function in acute ischemia, suggesting that δPKC may be involved in microvascular dynamics in the brain (Ramzy et al., 2006). In an *in vitro* preparation of rat posterior cerebral artery, δPKC activation was shown to mediate sustained intracellular calcium elevation via activation of cation channels, which in turn, caused sustained vasoconstriction (Kashihara et al., 2008). Administration of δV1-1 (a specific δPKC inhibitor preventing translocation to cellular membranes) after MCAO enhanced the number of patent vessels and significantly increased regional CBF detected by laser Doppler flowmetry (Bright et al., 2007). Unlike the detection of regional CBF via laser Doppler flowmetry, our method of detecting cerebral vascular dynamics after global cerebral ischemia (via ACA model) at the microvessel level utilizing *in vivo* 2-photon microscopy is highlighted in this study. In fact, microvessel-mediated CBF is functionally important and has not been well-characterized due to previous technological limitations. Therefore, the focus of this study was to determine 1) δPKC's effects on CBF in the presence of global cerebral ischemia, 2) cerebral vascular effects of δPKC before and after global cerebral ischemia, and 3) the role of δPKC in neuronal viability of the ischemic brain.

Experimental Procedures

Chemicals

δPKC inhibitor (δV1-1) and tat carrier peptide (control) (0.5 mg/kg, IV) were dissolved in sterile saline (0.9 %) (KAI Pharmaceuticals Inc., San Francisco, CA, USA). A final volume of 700 μl (Tat peptide or δV1-1) was injected intravenously (IV) 30 mins before induction of 2-vessel occlusion with hypotension (2-VO) or asphyxial cardiac arrest (ACA). Fluorescein-isothiocyanate-dextran (average MW, 2,000,000, Sigma Aldrich, St. Louis, MO) (0.2 mg/ml) was injected IV every 30 mins to visualize blood flow and microvessels.

δV1-1 inhibitor

Dr. Mochly-Rosen's laboratory at Stanford University has developed peptide inhibitors and activators of PKC function that act by competing with or inducing the association of individual PKC isozymes with their corresponding receptors of activated C kinases (RACKs). To introduce these PKC regulating peptides into cells, they used Antennapedia (Derossi et al., 1994; Theodore et al., 1995), Tat (Vives et al., 2007), or poly-arginine (Wender et al., 2000) carrier peptides to deliver the PKC regulating peptides into cells, with all methods yielding effective delivery (Gray et al., 1997; Dorn et al., 1999; Souroujon and Mochly-Rosen, 1998). We have fully corroborated the selectivity of these peptides as highly selective activators or inhibitors of two novel PKC isozymes (i.e. epsilon and delta) (Raval et al., 2005; Dave et al., 2005)

PKC Selectivity

The selectivity of δPKC inhibitor peptide δV1-1 has been previously shown by Chen et al., 2001 and Begley et al., 2004. In addition, Bright et al., 2004 showed that δV1-1 selectively inhibited δPKC translocation/activation *in vitro*, and has anti-apoptotic properties.

Animal Preparation

All experimental procedures were approved by the laboratory animal care and use committee (University of Miami, Miller School of Medicine). Male Sprague-Dawley rats weighing 250–350 g were fasted overnight and then anesthetized with 4 % isoflurane and a 30:70 mixture of oxygen and nitrous oxide followed by endotracheal intubation. Isoflurane was subsequently lowered to 1.5 % to 2 % for endovascular access. With the exception of resuscitation after ACA, 1.5 – 2 % isoflurane was administered to the animal throughout the time-course of these experiments. Administration of isoflurane in paralyzed animals is a well-established paradigm (Dave et al., 2006). The femoral vein was cannulated using a 20 gauge single-lumen polyethylene catheter. The femoral arteries were cannulated using a single-lumen (PE-50) catheter for continuous blood pressure monitoring and blood gas analyses. Plasma glucose levels (2300 stat plus, YSI) were determined before and after ischemia. Arterial blood gases (ABL-50, Radiometer) were measured intermittently (before ischemia, 10 and 30 min after ischemia) throughout the experiment. Goals were to maintain blood gases in the normal range (arterial pCO_2 = 35–40 mmHg, pO_2 ~ 120–140 mmHg). Physiological variables such as pH, pCO_2, O_2, and plasma glucose concentration were similar in tat and δV1-1-treated rats before and after ischemia. The rats were immobilized with pancuronium bromide for 2-VO (0.75 mg/kg, IV, administered every 15 min) and vecuronium bromide for ACA (2.0 mg/kg, IV, administered every 30 min) and maintained immobilized throughout the procedure.

Global Cerebral Ischemia (2-vessel occlusion, 2-VO)

Both common carotid arteries were exposed by a midline ventral incision and gently dissected free of surrounding nerve fibers. Ligatures of polyethylene (PE-10) tubing, containing double-lumen silastic tubing, were passed around each carotid artery. Systemic body temperature was maintained at 36-37°C throughout the experiment by a heating pad placed below the rat's body. Immediately prior to the ischemic insult, blood was gradually withdrawn from the femoral artery into a heparinized syringe to reduce systemic blood pressure to 45–50 mmHg throughout the duration of ischemia. Cerebral ischemia was produced by tightening the carotid ligatures bilaterally for 10 min. To allow post-ischemic reperfusion, the carotid ligatures were removed, and the shed blood re-injected into the femoral artery. This infusion usually restores mean arterial blood pressure (MABP) to normal range (120–140 mmHg) (Dave et al., 2008).

Asphyxial cardiac arrest (ACA)

Animals were prepared as described above. MABP and electrocardiogram (ECG) were continuously monitored. The data were recorded using iWorx 118 Research Grade Data Recorder and Labscribe Data Acquisition Software. The head and body temperatures were maintained at 36.5–37.0°C using heating lamps. The rats were immobilized with vecuronium bromide (2.0 mg/kg, IV, administered every 30 min) and maintained immobilized throughout the procedure with subsequent injections. To induce ACA, apnea was induced by disconnecting the ventilator from the endotracheal tube. 6 min after asphyxia, resuscitation was initiated by administering a bolus injection of epinephrine (0.005 mg/kg, IV) and sodium bicarbonate (1 meq/kg, IV) followed by mechanical ventilation with 100 % oxygen at a rate of 80 breaths/min and manual chest compressions until MABP reached 60 mm Hg and was maintained by the spontaneously beating heart for more than 10 s. After 10 min of restoration of spontaneous circulation (ROSC), the ventilator rate was decreased to 60 breaths/min and the oxygen lowered to 30 % in a mixture with N_2O. Arterial blood gases were then measured. If any corrections in

acid–base status were necessary, sodium bicarbonate was administered and/or the ventilator settings were adjusted. After ACA, the animal was placed directly onto the 2-photon microscopy (2-PM) stage with the stereotaxic device in place for cortical microvessel imaging for acute time points 15, 30, 45, and 60 min. Approximately 15 min was required to properly place the rat on the stereotaxic chamber and properly mount the rat on the 2-PM stage with all the necessary catheters and ECG lines. One limitation of the ACA model is the inability to detect the possible early hyperemia due to the inability to image via 2-PM from 0–14 min after ACA. Additional series of 2-PM imaging were performed on rats 4 and subsequently 24 hrs after ACA. For these experiments, the animal was allowed to recover and maintain hemodynamic stability by spontaneously breathing, usually by 10–15 min after ROSC, the catheters were removed and the animal extubated, and 100 % O_2 was delivered via face mask. Head and body temperatures were maintained at 37.0 °C using heating lamps 1 hr for recovery. Rats were then placed in a humidified incubator that maintained an ambient temperature of 29.0 °C for 12 hrs. Control animals (sham) were subjected to surgical procedure similar to ACA animals except induction of ACA. The resuscitation drugs were not used; however, sham animals were treated with isoflurane similar to experimental animals (Dave et al., 2006).

Thinned-Skull Window Method

The thinned-skull window method is a modified method from Xu et al., 2007. Anesthetized rats were placed on a stereotaxic frame to ensure the stability of the rat. After femoral arteries and vein of the rat were cannulated and carotid ligatures installed, a longitudinal incision extending from the neck region to the frontal area of the rat was made at the midline scalp using microsurgical tools. Utilizing a high-speed micro-drill, a thin circular area of the skull (approximately ~ 2 mm in diameter) was made 1 mm from bregma. Thinned-skull window was created carefully with the micro-drill thinning out the skull with constant irrigation with sterile saline as to not overheat the skull or the drill bit. The skull is thin enough for visualization of blood vessels via 2-PM when it is approximately half the thickness of the skull or approximately 0.5 mm (Xu et al., 2007).

Two-photon Microscopy (2-PM)

After thinning the skull, the rat was placed on a 2-PM (Lasersharp2000, BioRad, Hercules, CA). pH, mean arterial blood pressure, pCO_2, pO_2, glucose, rectal and head temperatures were constantly monitored throughout the experiment. Head temperature was determined by a thermocoupler implanted in the temporalis muscle upon incision (Dietrich et al., 1993). Sterilized water (0.5 ml) was added on top of the thinned-skull window. A 20 X water immersion objective (Olympus XLUMPlanFl) was lowered in proximity to the thinned-skull window. The objective (heated by circulating water jacket), in contact with sterilized water, provides temperature regulation of the skull. Fluorescent images were captured at an excitation wavelength of 910 nm with the intravenous introduction of fluorescein-dextran. Cortical cerebral blood vessel images were captured at 20 X, and 200 X. Additionally, Z-series (20 X) and linescan (200 X) images were obtained throughout the time course of the experiment at t = 0, 30 min after drug treatment (tat peptide or δV1-1), and 5, 15, 30, 45, and 60 min after 10 min of 2-VO. For ACA studies, images were captured t = 0, 30 min after drug treatment (tat peptide or δV1-1), and 15, 30, 45, 60, 240 min (4 hrs), 1440 min (24 hrs) after ACA (the last two groups in a separate series of animals). Only microvessels with diameters 5–10 μm were considered for 2-photon microscopy studies. Upon visual inspection, arterioles can be recognized morphologically based on arterioles branching out from larger vessels, while, venules merge into larger vessels as defined by Koike et al., 2004.

Linescans for red blood cell (RBC) velocities and blood vessel diameter measurements were analyzed with Image J analysis software (Nishimura et al., 2007). Each velocity measurement was calculated by measuring the slope of the dark lines (5–10 lines) representing 5–10 RBC

traversing at a point in time of the linescan. The slopes were calculated and averaged. One microvessel was studied per rat with an overall diameter on average of 10 μm. Our data were expressed as percent change in flow or blood vessel diameter. This was achieved by utilizing each rat as its own internal control. Baseline measurements before ischemia or drug treatment were used for normalization of the data. This analysis was necessary due to the fact that not all microvasculature possess exactly the same vessel size or RBC velocities before ischemia and/or drug treatments.

Western Blot Analysis

Brain tissue was fractionated as previously described (Raval et al., 2005). In brief, 24 hours after ACA, the animals were sacrificed and the cortex (site of 2-PM observed CBF) was suspended in 400 μl of lysis buffer (4 mM ATP, 100 mM KCl, 10 mM imidazole, 2 mM EGTA, 1 mM $MgCl_2$, 20 % glycerol, 0.05 % Triton X-100, 17 μg/ml phenylmethylsulfonyl fluoride, 20 μg/ml soybean trypsin inhibitor, 25 μg/ml leupeptin, and 25 μg/ml aprotinin) and homogenized using a glass homogenizer. The homogenate was centrifuged at 1000×*g* for 10 min at 4°C. The resulting pellet (membrane fraction) was resuspended in lysis buffer containing 1 % Triton X-100. [When δPKC is activated, it is translocated from the cytosol to the membrane (particulate). Therefore, the membrane fraction is probed for δPKC.] Equal amounts of protein were separated on a 10 % SDS-PAGE gel and electroblotted to nitrocellulose. Membranes were blocked in 5 % milk/TBS-T and hybridized with anti- δPKC rabbit polyclonal antibody (Santa Cruz Biotechnology, Santa Cruz, CA) overnight at 4°C. Proteins were detected by anti-rabbit horse-radish peroxidase conjugated secondary antibody and enhanced chemiluminescence (ECL) system (Pierce Thermo Scientific, Rockford, IL). Protein loading was determined by re-probing the membrane for glyceraldehydes 3-phosphate dehydrogenase (GAPDH) (anti-GAPDH mouse monoclonal antibody) from Advanced Immunochemical Inc, Long Beach, CA. Western blot densitometry was analyzed using Image J software from the NIH.

Histopathology

In a separate series of animals, 7 days after ACA insults, rats were anesthetized with isofluorane, perfused for 1 min with physiologic saline, a mixture of 40 % formaldehyde, glacial acetic acid, and methanol, (FAM) 1:1:8 (vol/vol/vol) for 19 min. Histopathology was performed only on ACA-treated animals due to the fact that it is a more clinically relevant model of global cerebral ischemia. The perfusate solution was delivered into the root of the ascending aorta at a constant pressure of 110–120 mm Hg, as described previously (Dietrich et al., 1993). The head was removed and immersed in FAM at 4 °C for 1 day. The brain was removed from the skull, and coronal brain blocks were embedded in paraffin. Coronal sections of 10 μm thickness were stained with hematoxylin and eosin (Perez-Pinzon et al., 1997). CA1 hippocampal sections were stained with hematoxylin and eosin and visualized at 40 X magnification with a Nikon Microphot-SA microscope equipped with a Sony CCD camera interfaced to a MCID image analyzer (Imaging Research, Ontario, Canada). An investigator blinded to the experimental conditions in both the sham and ACA groups counted ischemic neurons, 18 fields per section, along the medial to lateral extent of the CA1 region of the hippocampus 3.8 mm posterior to the bregma. The ischemic neuronal changes consist of severe cellular shrinkage, cytoplasmic eosinophilia, pyknotic triangular-shaped nucleus with dark basophilic staining, and eosinophilic staining nucleolus, as described previously (Perez-Pinzon et al., 1997).

In the same series of animals, rat brain sections spanning the subfornical organ (SFO) were analyzed to assess cortical neuronal damage 7 days after ACA. This region was determined to be −1.4 mm to −0.8 mm with respect to bregma, similar to the location where 2-PM imaging of cortical microvessels was analyzed. Rat brain slices were excised, paraffin embedded, and

stained for hematoxylin and eosin as already mentioned. Every tenth section spanning the desired region was collected, totaling of 6 samples per side spanning the entire SFO region. Cell counting was performed using a software analyzer (MCID elite) coupled to a light microscope as already mentioned. Rat cortex sections spanning the SFO region were viewed under 10 X magnification. A region between 3,000,000 and 4,000,000 μm^2 was traced using the software program, which contained cortical layers II, III, and IV. This region was then sampled under 40 X magnification. A sampling frequency of 2 % was selected, with each field containing an area of 20,000 μm^2. This translated to 30 fields per selected region. As each field was analyzed, the number of dead neurons in the sample space were counted, recorded, and totaled. This procedure was then repeated with two other slides from the same animal and repeated for the contralateral hemisphere. The total number of dead neurons selected through this sampling technique was used to estimate total dead neuronal population in the entire cortical region of the rat (Burke et al., 2009).

The total volume of cortical tissue was determined by using the average area of the selected region of all three slides for one hemisphere. This was multiplied by the breadth of the SFO region (~ 600 μm). The total number of counted dead neurons from the previous procedure was normalized to cortical volume selected in the cortical region. The final values are expressed as number of dead neurons per cubic millimeter of cortical tissue.

Statistical Analysis

Results were expressed as means ± S.E.M. Statistical analysis was evaluated by Student's *t* test for paired or unpaired samples or one-way ANOVA followed by Tukey's *post hoc* test as appropriate with SPSS statistical software (Chicago, IL). The $p \leq 0.05$ level of probability was accepted as significant.

Results

δV1-1 Blunts Hyperemia and Hypoperfusion in Cortical Microvessels after 2-VO

Representative images of cortical microvasculature are shown in Figure 1A–1B. Linescans of red blood cells (RBC) traversing the microvasculature were measured (Figure 1C) and summarized in Figure 1D. Black shadows traveling from left to right indicate RBC flow across the scanned vessel. A less negative slope (rise/run) represents RBC (baseline) traveling at a faster rate [e.g., tat peptide (vehicle), 10 min after ischemia], whereas a more negative slope represents RBC traveling at a slower rate (e.g., tat peptide, 60 min after ischemia). After each linescan, microvessel images were captured to measure overall microvessel diameter (Figure 1B–1E). Rats pretreated with δV1-1 for 30 min significantly attenuated hyperemia (less than 75 % change in flow at 5, and 15 min) after 2-VO (Figure 1D). At the cortical microvessel level, we also observed amelioration of hypoperfusion by inhibition of δPKC (less than 75 % change in flow at 45 and 60 min after 2-VO) (Figure 1D). In the presence of δV1-1, post-ischemic hyperemia and hypoperfusion suggest cortical microvessel vasoconstriction (less than - 20 % change in blood vessel diameter 5 and 10 min with δV1-1 treated animals) followed by vasodilation (greater than 10 % change in blood vessel diameter 45 and 60 min with δV1-1 treated animals) after 2-VO (Figure 1E) (n = 4 – 6, * $p \leq 0.05$). The CBF monitored by 2-PM measured single microvessels in the cerebral cortex (pre and post 2-VO), while laser-Doppler flowmetry (LDF) measured regional CBF at a given time (pre and post-2-VO). δV1-1 pretreatment significantly attenuated hyperemia 5 min after 2-VO (52 % ± 28 increase in flow measured by LDF) (data not shown). Our findings with these two techniques produced similar results suggesting that 2-PM method of measuring CBF is similar or correlative to the LDF method, with better resolution at the microvessel level.

δV1-1 Improves Perfusion in Cortical Microvessels after ACA

Cortical microvessel experiments were performed after 6 min of ACA. In contrast to the 2-VO studies, statistically significant changes in cortical microvessel blood flow in rats pretreated with δV1-1 after ACA were not detected. Animals without any drug (control) or tat peptide pretreatment exhibited a decrease in RBC flow 15–60 min after 6 min of ACA. Although not statistically significant, rats pretreated with δV1-1 enhanced RBC flow 15 and 30 min after ACA (−30 % ± −9.8 % and −2.4 % ± 15 % increase in flow as compared to control or tat peptide, respectively.) and decreased RBC flow 45 and 60 min after ACA (−28 % ± −9.2 % and −17 % ± −7.3 % decrease in flow as compared to control or tat peptide, respectively.) (Figure 2A). A decrease in cortical microvessel diameter was detected 60 min after ACA (−20 % ± −10 % decrease in diameter as compared to control or tat peptide.), but was not statistically significant (Figure 2B) (n = 3 – 6, * p 0.≤ 05).

Next, in a separate set of animals, we measured CBF changes with the 2-PM technique at 4 and 24 hrs after ACA in the presence or absence of δV1-1. No significant change in CBF was detected at 4 hrs after ACA as compared to control or tat peptide. However, rats pretreated with δV1-1 enhanced CBF 24 hrs after ACA (160 % ± 55 % increase in flow 24 hrs after ACA as compared to control or tat peptide) (Figure 2C). Unlike the 2-VO studies, this increase in blood flow was not associated with an increase in blood vessel diameter (Figure 2D) (n = 6, * $p \leq 0.05$).

Since δV1-1 pretreatment may be protecting the brain parenchyma against the deleterious effects of the ischemic insult, in a separate set of experiments, δV1-1 was administered directly after ACA and CBF changes were monitored using the 2-PM method. CBF was enhanced in the presence of δV1-1 post-arrest, (121 % ± 47 % and 94 % ± 20 % increase in CBF 45 and 60 min after ACA, respectively, as compared to tat peptide) (Figure 2E) but no significant changes in blood vessel diameters were detected (Figure 2F) (n = 4 – 6, * $p \leq 0.05$). Physiological parameters are provided in Table 1. The pH of the animals was reduced while the partial pressure of oxygen (PO_2) for all groups (After ACA) were greater than 150 mmHg, due to 100 % delivery of oxygen and increased ventilator rate (60 breaths/min to 80 breaths/min) during and after resuscitation. No significant results were observed in any physiological parameters 4 and 24 hrs after ACA. These results suggest that post-treatment with δV1-1 attenuated ACA-induced hypoperfusion.

δV1-1 Inhibits δPKC Translocation in the Cortex

Next, we determined if pretreatment with δV1-1 inhibits δPKC translocation when subjected to ACA. 24 hrs after ACA, rats were sacrificed and cortices (site of 2-PM observed CBF) were extracted for Western blot analyses. Our results showed that pretreatment with δV1-1 in the rat inhibited δPKC translocation after ACA (Figure 3A) with a 61 % reduction as compared to tat peptide (vehicle) treatment (Figure 3B) (n = 4 – 6, * $p \leq 0.05$). Physiological parameters are provided in Table 2. PO_2 for all groups (After ACA) were greater than 150 mmHg, due to 100 % delivery of oxygen and increased ventilator rate (60 breaths/min to 80 breaths/min) during and after resuscitation. These results further confirm that δV1-1 inhibits translocation of δPKC to the cellular membrane in the brain, rendering δPKC inactive.

δV1-1 Confers Neuroprotection after ACA

Our data suggest a prominent role for δPKC on CBF derangements after ACA and 2-VO models of global cerebral ischemia; therefore, we tested the hypothesis that δPKC promotes neuronal cell death following 6 min of ACA. Sham operated experimental group (1023 ± 11 normal neurons in CA1 region of the hippocampus) was used as control. Rats pretreated with δV1-1 afforded neuroprotection (813 ± 62 normal neurons) in the CA1 region of the rat hippocampus

7 days after 6 min of ACA, as compared to tat peptide-treated animals (639 ± 20 normal neurons) and control (527 ± 19 normal neurons).

Since cortical cerebral blood flow was measured throughout this study, we determined the number of dead cortical neurons in the same region as CBF measurements performed using the 2-PM method. Rats pretreated with δV1-1 (3187 ± 458.0 dead neurons) afforded neuroprotection suggesting a decrease number of dead cortical neurons as compared to no drug (8400 ± 1621 dead neurons) and tat peptide (6863 ± 645.5 dead neurons) experimental groups (Figure 4) ($n = 3 – 7$, * $p \leq 0.05$). Physiological parameters are provided in Table 3. As in previous experiments (Table 1), the pH of some animals was slightly reduced while the PO_2 for all groups (After ACA) were greater than 148 mmHg, due to 100 % delivery of oxygen and increased ventilator rate (60 breaths/min to 80 breaths/min) during and after resuscitation. These results suggest that δPKC is intimately involved in neuronal cell viability in the hippocampus as well as in cortex.

Discussion

Biphasic Changes of Cerebral Blood Flow

The role of δPKC as it relates to cerebral circulation has not been well characterized. Our data suggest that δPKC is intimately involved in the induction of hyperemia and hypoperfusion after global cerebral ischemia. δPKC is intimately involved in cortical cerebral circulation by modulating post-ischemic CBF by attenuating hyperemia and hypoperfusion. This was characterized by a decrease in CBF (15 min after 2-VO) with a subsequent increase (45 min after 2-VO) in the presence of δV1-1 pretreated rats 30 min before ischemia (Figure 1D). This attenuation of hyperemia and hypoperfusion in the presence of δV1-1 also resulted in cortical blood vessel diameters to decrease (vasoconstriction) during hyperemia and increase (vasodilation) during hypoperfusion measured by 2-PM (Figure 1E). Although other vasoactive mediators may be involved in hyperemia and hypoperfusion, it is thought to be largely regulated by nitric oxide (NO) (a potent vasodilator) (Humphreys and Koss, 1998) and endothelin (ET, a potent vasoconstrictor) (Dawson et al., 1999), respectively.

Cerebral Blood Flow Determination

It is important to note that blood flow is defined as ml/min/kg (Pu et al., 2004). We measured RBC velocities via 2-PM, also known as speed (distance/time) or flux (Kleinfeld et al., 1998), without considering direction. However, we do not take into consideration RBCs that changed direction during the course of these experiments. This is a minor caveat of this technique and thus, we cannot definitely suggest that any changes in flow observed by 2-PM, is blood flow per se. We propose that changes observed by this technique are highly suggestive of changes in blood flow. In addition, the similarities of our initial CBF studies with LDF further suggest that our 2-PM data is closely linked to CBF. For the sake of clarity, we considered “flow” throughout the entire course to be proportional to speed.

Global Cerebral Ischemia Models

The overall goal in our laboratory is to determine the pathophysiological mechanisms in a clinically relevant model (via ACA). However, it is important to note that acute hyperemia of the ACA-treated rat cannot be measured using the 2-PM method due to the fact that it takes approximately 15 min to properly place the rat on the stereotaxic chamber and properly mount it on the 2-PM stage with all the necessary catheters and electrocardiogram lines after ACA. The limitation of the ACA model is the inability to detect the possible early hyperemia due to the inability to image by 2-PM from 0–14 min after ACA. Therefore, we used the 2-VO method to detect acute hyperemia and hypoperfusion up to 60 min after ischemia. 2-VO with 2-PM visualization of cortical blood vessels was performed with an intubated rat on the 2-PM

microscope stage. A caveat for the 2-VO model in the 2-PM setup is that animal survival for many hours after ischemia is not feasible due to poor survival of animals after 2-VO and subsequent 2-PM imaging session. Therefore, for long-term 2-PM measurements (4 and 24 hrs after ischemia) we only used the ACA model. Initial 2-VO experiments led to subsequent, more focused studies using 2-PM to examine individual microvessels in ACA-treated animals.

In our global cerebral ischemia experiments, we administered 0.5 mg/kg, IV of δV1-1 or tat peptide (vehicle control). Our dosage is based on the report from Bright et al., 2007, where they administered 0.2 mg/kg, IP of tat peptide or δV1-1. This discrepancy is due to the difference in the route of administration. The difference in route of administration is necessary, due to the fact that once the animal is secured on the stereotaxic chamber; movement of the animal is avoided to insure accurate measurements of CBF. From our experience, 0.5 mg/kg, IV is effective in inhibiting neuronal cell death in the CA1 region of the hippocampus, and thus we used it in the current study. This concentration is also within safety levels previously determined (Souroujon and Mochly-Rosen, 1998).

Our current findings suggest that a strong correlation between CBF and cortical blood vessel diameter modulation in the 2-VO but not ACA model of global cerebral ischemia in the presence of δV1-1 (Figures 1 and 2). Unlike 2-VO, it is plausible that the ACA model of global cerebral ischemia promotes neurovascular uncoupling, which may cause dysregulation in vascular tone by modulation of blood vessel diameters independent of local CBF. In contrast, it is likely that neurovascular coupling is still maintained in the 2-VO model of global cerebral ischemia by direct evidence of correlative blood vessel diameters v. blood flow. Our results demonstrate that there is a significant difference between the two models of global cerebral ischemia. Since ACA is a more clinically relevant model of cerebral ischemia after cardiac arrest, it was important to define this difference.

Vasoactive mediators regulating hyperemia and/or hypoperfusion after global cerebral ischemia have been suggested, but direct evidence *in vivo*, have not been demonstrated. NO, a gasotransmitter, is known to cause both potent vasodilation and neurotransmission derived from perivascular nerves (Si and Lee, 2002). ET, a 21-amino acid peptide, is a potent vasoconstrictor (Yanagisawa et al., 1988). ET also indirectly modulates NO release through other signal transduction pathways such as PKC (Henriksson et al., 2007). NO and ET have been suggested to be up-regulated during ischemia/reperfusion injury (Humphreys and Koss, 1998; Dawson et al., 1999) and may be responsible for enhanced hyperemia and hypoperfusion, respectively (Humphreys and Koss, 1998; Dawson et al., 1999). This suggests a disruption of the delicate balance among potent vasodilators and vasoconstrictors in cerebral circulation after ischemia (Hosomi et al., 2007).

Adenosine (a well-established vasodilator), may also be involved in the ischemia-induced hyperemia. During ischemia, the accumulation of adenosine is enhanced as ATP is depleted. Since adenosine is also a potent vasodilator, this overabundance of adenosine is thought to also be responsible for ischemia-induced hyperemia (Sciotti and Wylen, 1993). Consequences of ischemia-induced hypoperfusion also include delayed neuronal cell death (Hossmann, 1993) in selective vulnerable CA1 region of the hippocampus.

Using ACA, as a cardiac arrest model, we showed that δPKC was involved in cortical CBF reduction even 24 hrs after ACA. This hypoperfusion was ameliorated by pretreatment with δV1-1, which occurred with no significant changes in blood vessel diameters. In contrast, in the 2-VO model of global cerebral ischemia, there was a good correlation between RBC velocity and microvessel diameter (Figures 1D and 1E). This type of discrepancy between changes in cortical RBC velocity vs microvessel diameters was previously shown by Kleinfeld et al., 1998 and Nishimura et al., 2007 under normal CBF conditions. Thus, we surmise that

cerebral ischemia may promote neurovascular uncoupling, which may help explain the dysregulation in vascular tone by modulation of blood vessel diameters independent of local CBF after ACA. This dysregulation may arise from intrinsic pathologies of cerebral vessels. Since our results with δV1-1 pretreatment could be explained by δPKC acting on protecting the parenchyma itself and thus causing indirect CBF derangements, we studied the effects of δPKC post-treatment on CBF after ACA. These data (Figure 2E) suggest that δPKC is directly modulating CBF after ACA. This assertion is further confirmed by our results in which administration of δV1-1 at 24 hrs after ACA was able to reverse hypoperfusion even at that late stage of reperfusion. In humans, hypoperfusion 24 hrs after cardiac arrest and restoration of spontaneous circulation (ROSC) is associated with poor prognosis and rate of recovery (Roine et al., 1991; Oku et al., 1993). The lack of successful treatment modalities (Oku et al., 1993) adds further clinical relevance to our findings. In fact, the significance of elucidating the mechanism of how δPKC affects CBF after cardiac arrest is further emphasized by the fact that Phase II clinical trials are underway to test the safety and efficacy of the δPKC inhibitor peptide (KAI-9803; Kai Pharmaceuticals, San Francisco, CA) in acute myocardial infarction (Bates et al., 2008).

Another potential target for δPKC's effect on inducing CBF derangements after cerebral ischemia is the endothelial cells. The viability and function of endothelial cells is greatly affected by ischemia. For example, δPKC inhibition preserved coronary endothelial cell function and vasodilator capacity in acute myocardial infarction (Kaneda et al., 2009). Although this was in systemic circulation, we conjecture that this could hold great significance when extended to cerebral vasculature. We suspect that δPKC's functional targets are not only directed at one or two cell types within the neurovascular unit, but affect multiple cell types within the neurovascular unit to alter CBF.

Our findings suggest that other factors may be involved in ACA-induced disruption of cortical CBF (i.e. neurovascular uncoupling between effector cell types and the vascular smooth muscle or other downstream mediators regulating vascular tonicity), further illustrating the important differences between the two models (ACA vs 2-VO) of global cerebral ischemia. We demonstrated that disruption of cortical CBF via ACA directly affects cortical neuron viability (Figure 4). This may be extended to other parts of the brain causing potential detrimental effects. For example, δV1-1 pretreated rats exhibited neuroprotection in the CA1 region of the hippocampus 7 days after ACA, while control (no drug treatment) rats presented a 49 % loss in neuronal viability (see Results). These results suggest that inhibition of δPKC ameliorates CBF derangements that may otherwise lead to neuronal loss after cerebral ischemia (Churchill et al., 2007). In addition, we can infer that the neuroprotective effects of δV1-1 may be attributed to latent enhancement in CBF 24 hrs after ACA, thus preserving neurons otherwise susceptible to ischemic damage.

Current studies have suggested the multi-faceted effects of δPKC after cerebral ischemia. In the context of neuroprotection and ischemic injury, ACA or organotypic hippocampal slices treated with oxygen-glucose deprivation enhanced cytochrome c and caspase 3 activation promoted δPKC translocation resulted in neuronal cell death (Raval et al., 2005). Others have reported that δPKC activation induced cell death through caspase 3 activation resulting in cellular apoptosis in cardiac ischemia/reperfusion injury (Churchill et al., 2007). This is corroborated by our current findings indicating that δV1-1 inhibited δPKC translocation in cortical lysates suggesting the presence and function of δPKC after ACA (Figure 3) promotes neuroprotection in the hippocampus and cortex. Rats treated with δV1-1 resulted in enhanced CBF after MCAO and improved cerebrovascular pathology (Bright et al., 2007). In addition, experiments with δPKC knock-out mice suggested that δPKC contributed to damage by enhancing inflammatory mediators after transient focal ischemia reducing infarct volumes and neutrophil invasion as compared to wild-type (Chou et al., 2004).

Conclusions

To our knowledge, an in-depth investigation of the role of δPKC on cerebral circulation in the 2-VO and ACA models of global cerebral ischemia has not been well understood. Our data suggest that δPKC is involved in mediating both hyperemia and hypoperfusion phases during reperfusion after global cerebral ischemia. Thus, δV1-1 can be used to reduce cerebral ischemic injury. In addition, δV1-1 can modulate postischemic blood flow/vessel dynamics that may be beneficial in the treatment of cerebral ischemia. Except for hypothermia (Dietrich et al., 1993), all neuroprotective trials for cardiac arrest have been unsuccessful and therefore, new pharmacological interventions are greatly needed. One of the main challenges in developing effective post-ischemic therapy is extending the therapeutic time window. Using in vivo models of cerebral ischemia, we have demonstrated that δPKC is activated following cardiac arrest. When activation of δPKC is attenuated with a peptide inhibitor, the brain is protected from ischemic damage (Bright et al., 2004 and 2007; Raval et al., 2005) through possible revival and/or stabilization of cerebral circulation. The therapeutic potential by targeting δPKC may prove beneficial in patients with cardiac arrest-induced CBF derangements. This is underscored by the fact that δPKC inhibitors are currently in phase II clinical trials for acute myocardial infarction.

Acknowledgments

This work was supported by National Institutes of Health grants NS45676-01, NS054147-01, NS34773, T32-NS007459-10, and American Heart Association grant 10POST4340011. Tat peptide and δPKC inhibitor (δV1-1) were purchased from KAI Pharmaceuticals Inc., San Francisco, CA, USA.

References

Bates E, Bode C, Costa M, Gibson CM, Granger C, Green C, Grimes K, Harrington R, Huber K, Kleiman N, Mochly-Rosen D, Roe M, Sadowski Z, Solomon S, Widimsky P. Intracoronary KAI-9803 as an adjunct to primary percutaneous coronary intervention for acute ST-segment elevation myocardial infarction. Circulation 2008;117:886–896. [PubMed: 18250271]

Begley R, Liron T, Baryza J, Mochly-Rosen D. Biodistribution of intracellularly acting peptides conjugated reversibly to Tat. Biochem Biophys Res Commun 2004;318:949–954. [PubMed: 15147964]

Bright R, Raval AP, Dembner JM, Pérez-Pinzón MA, Steinberg GK, Yenari MA, Mochly-Rosen D. Protein kinase C delta mediates cerebral reperfusion injury in vivo. J. Neurosci 2004;24:6880–6888. [PubMed: 15295022]

Bright R, Steinberg GK, Mochly-Rosen D. Delta PKC mediates microcerebrovascular dysfunction in acute ischemia and in chronic hypertensive stress in vivo. Brain Res 2007;1144:146–155. [PubMed: 17350602]

Brodie C, Blumberg PM. Regulation of cell apoptosis by protein kinase c delta. Apoptosis 2003;8:19–27. [PubMed: 12510148]

Burke M, Zangenehpour S, Mouton PR, Ptito M. Knowing what counts: Unbiased stereology in the non-human primate brain. J Vis Exp 2009;27

Caplan LR, Wong KS, Gao S, Hennerici MG. Is hypoperfusion an important cause of strokes? If so, how? Cerebrovasc Dis 2006;21:145–153. [PubMed: 16401883]

Chen L, Hahn H, Wu G, Chen CH, Liron T, Schechtman D, Cavallaro G, Banci L, Guo Y, Bolli R, Dorn GW II, Mochly-Rosen D. Opposing cardioprotective actions and parallel hypertrophic effects of delta PKC and epsilon PKC. Proc Natl Acad Sci USA 2001;98:11114–11119. [PubMed: 11553773]

Choi BH. Oxygen, antioxidants and brain dysfunction. Yonsei Med J 1993;34:1–10. [PubMed: 8379180]

Chou WH, Choi DS, Zhang H, Mu D, McMahon T, Kharazia VN, Lowell CA, Ferriero DM, Messing RO. Neutrophil protein kinase Cdelta as a mediator of stroke-reperfusion injury. J Clin Invest 2004;114:49–56. [PubMed: 15232611]

Churchill EN, Mochly-Rosen D. The roles of PKCdelta and epsilon isoenzymes in the regulation of myocardial ischaemia/reperfusion injury. Biochem Soc Trans 2007;35:1040–1042. [PubMed: 17956273]

Dave KR, Lange-Asschenfeldt C, Raval AP, Prado R, Busto R, Saul I, Pérez-Pinzón MA. Ischemic preconditioning ameliorates excitotoxicity by shifting glutamate/gamma-aminobutyric acid release and biosynthesis. J Neurosci Res 2005;82:665–673. [PubMed: 16247804]

Dave KR, Raval AP, Purroy J, Kirkinezos IG, Moraes CT, Bradley WG, Perez-Pinzon MA. Aberrant deltaPKC activation in the spinal cord of Wobbler mouse: a model of motor neuron disease. Neurobiol Dis 2005;18:126–133. [PubMed: 15649703]

Dave KR, Saul I, Prado R, Busto R, Perez-Pinzon MA. Remote organ ischemic preconditioning protect brain from ischemic damage following asphyxial cardiac arrest. Neurosci Lett 2006;404:170–175. [PubMed: 16781056]

Dave KR, DeFazio RA, Raval AP, Torraco A, Saul I, Barrientos A, Perez-Pinzon MA. Ischemic preconditioning targets the respiration of synaptic mitochondria via protein kinase C epsilon. J Neurosci 2008;28:4172–4182. [PubMed: 18417696]

Dawson DA, Sugano H, McCarron RM, Hallenbeck JM, Spatz M. Endothelin receptor antagonist preserves microvascular perfusion and reduces ischemic brain damage following permanent focal ischemia. Neurochem Res 1999;24:1499–1505. [PubMed: 10591398]

Derossi D, Joliot AH, Chassaing G, Prochiantz A. The third helix of the Antennapedia homeodomain translocates through biological membranes. J Biol Chem 1994;269:10444–10450. [PubMed: 8144628]

Dietrich WD, Busto R, Alonso O, Globus MY, Ginsberg MD. Intraischemic but not postischemic brain hypothermia protects chronically following global forebrain ischemia in rats. J Cereb Blood Flow Metab 1993;13:541–549. [PubMed: 8314910]

Dorn GW II, Souroujon MC, Liron T, Chen CH, Gray MO, Zhou HZ, Csukai M, Wu G, Lorenz JN, Mochly-Rosen D. Sustained in vivo cardiac protection by a rationally designed peptide that causes epsilon protein kinase C translocation. Proc Natl Acad Sci U S A 1999;96:12798–12803. [PubMed: 10536002]

Gray MO, Karliner JS, Mochly-Rosen D. A selective epsilon-protein kinase C antagonist inhibits protection of cardiac myocytes from hypoxia-induced cell death. J Biol Chem 1997;272:30945–30951. [PubMed: 9388241]

Henriksson M, Stenman E, Vikman P, Edvinsson L. MEK1/2 inhibition attenuates vascular ETA and ETB receptor alterations after cerebral ischaemia. Exp Brain Res 2007;178:470–476. [PubMed: 17091294]

Hosomi N, Ohyama H, Ichihara S, Takahashi T, Naya T, Kohno M. Relation of postischemic delayed hypoperfusion and cerebral edema after transient forebrain ischemia. J Stroke Cerebrovasc Dis 2007;16:103–108. [PubMed: 17689403]

Hossmann KA. Ischemia-mediated neuronal injury. Resuscitation 1993;26:225–235. [PubMed: 8134701]

Hossmann KA. Reperfusion of the brain after global ischemia: hemodynamic disturbances. Shock 1997;8:95–101. [PubMed: 9261898]

Humphreys SA, Koss MC. Role of nitric oxide in post-ischemic cerebral hyperemia in anesthetized rats. Eur J Pharmacol 1998;347:223–229. [PubMed: 9653886]

Kaneda H, Ikeno F, Inagaki K, Mochly-Rosen D. Preserved coronary endothelial function by inhibition of delta protein kinase C in a porcine acute myocardial infarction model. Int J Cardiol 2009;133:256–259. [PubMed: 18242734]

Kashihara T, Nakayama K, Ishikawa T. Distinct roles of protein kinase C isoforms in myogenic constriction of rat posterior cerebral arteries. J Pharmacol Sci 2008;108:446–454. [PubMed: 19057126]

Kleinfeld D, Mitra PP, Helmchen F, Denk W. Fluctuations and stimulus-induced changes in blood flow observed in individual capillaries in layers 2 through 4 of rat neocortex. Proc Natl Acad Sci U S A 1998;95:15741–15746. [PubMed: 9861040]

Koike N, Fukumura D, Gralla O, Au P, Schechner JS, Jain RK. Tissue engineering: creation of long-lasting blood vessels. Nature 2004;428:138–139. [PubMed: 15014486]

Koller A, Bagi Z. Nitric oxide and H2O2 contribute to reactive dilation of isolated coronary arterioles. Am J Physiol Heart Circ Physiol 2004;287:H2461–H2467. [PubMed: 15319207]

Nishimura N, Schaffer CB, Friedman B, Lyden PD, Kleinfeld D. Penetrating arterioles are a bottleneck in the perfusion of neocortex. Proc Natl Acad Sci U S A 2007;104:365–370. [PubMed: 17190804]

Oku K, Sterz F, Safar P, Johnson D, Obrist W, Leonov Y, Kuboyama K, Tisherman SA, Stezoski SW. Mild hypothermia after cardiac arrest in dogs does not affect postarrest multifocal cerebral hypoperfusion. Stroke 1993;24:1590–1597. [PubMed: 8378966]

Pérez-Pinzón MA, Xu GP, Dietrich WD, Rosenthal M, Sick TJ. Rapid preconditioning protects rats against ischemic neuronal damage after 3 but not 7 days of reperfusion following global cerebral ischemia. J Cereb Blood Flow Metab 1997;17:175–182. [PubMed: 9040497]

Pu X, Lee LS, Galinsky RE, Carlson GP. Evaluation of a rat model versus a physiologically based extraction test for assessing phenanthrene bioavailability from soils. Toxicol Sci 2004;79:10–17. [PubMed: 14976340]

Ramzy D, Rao V, Tumiati LC, Xu N, Sheshgiri R, Miriuka S, Delgado DH, Ross HJ. Elevated endothelin-1 levels impair nitric oxide homeostasis through a PKC-dependent pathway. Circulation 2006;114:I319–I326. [PubMed: 16820593]

Raval AP, Dave KR, Prado R, Katz LM, Busto R, Sick TJ, Ginsberg MD, Mochly-Rosen D, Pérez-Pinzón MA. Protein kinase C delta cleavage initiates an aberrant signal transduction pathway after cardiac arrest and oxygen glucose deprivation. J Cereb Blood Flow Metab 2005;25:730–741. [PubMed: 15716854]

Roine RO, Launes J, Nikkinen P, Lindroth L, Kaste M. Regional cerebral blood flow after human cardiac arrest. A hexamethylpropyleneamine oxime single photon emission computed tomographic study. Arch Neurol 1991;48:625–629. [PubMed: 2039385]

Sciotti VM, Van Wylen DG. Attenuation of ischemia-induced extracellular adenosine accumulation by homocysteine. J Cereb Blood Flow Metab 1993;13:208–213. [PubMed: 8436612]

Si ML, Lee TJ. Alpha7-nicotinic acetylcholine receptors on cerebral perivascular sympathetic nerves mediate choline-induced nitrergic neurogenic vasodilation. Circ Res 2002;91:62–69. [PubMed: 12114323]

Souroujon MC, Mochly-Rosen D. Peptide modulators of protein-protein interactions in intracellular signaling. Nat Biotechnol 1998;16:919–924. [PubMed: 9788346]

Theodore L, Derossi D, Chassaing G, Llirbat B, Kubes M, Jordan P, Chneiweiss H, Godement P, Prochiantz A. Intraneuronal delivery of protein kinase C pseudosubstrate leads to growth cone collapse. J Neurosci 1995;15:7158–7167. [PubMed: 7472470]

Vives E, Brodin P, Lebleu B. A truncated HIV-1 Tat protein basic domain rapidly translocates through the plasma membrane and accumulates in the cell nucleus. J Biol Chem 1997;272:16010–16017. [PubMed: 9188504]

Watson BD, Ginsberg MD. Ischemic injury in the brain. Role of oxygen radical-mediated processes. Ann NY Acad Sci 1989;559:269–281. [PubMed: 2549830]

Wender PA, Mitchell DJ, Pattabiraman K, Pelkey ET, Steinman L, Rothbard JB. The design, synthesis, and evaluation of molecules that enable or enhance cellular uptake: peptoid molecular transporters. Proc Natl Acad Sci U S A 2000;97:13003–13008. [PubMed: 11087855]

Xu HT, Pan F, Yang G, Gan WB. Choice of cranial window type for in vivo imaging affects dendritic spine turnover in the cortex. Nat Neurosci 2007;10:549–551. [PubMed: 17417634]

Yanagisawa M, Kurihara H, Kimura S, Tomobe Y, Kobayashi M, Mitsui Y, Yazaki Y, Goto K, Masaki T. A novel potent vasoconstrictor peptide produced by vascular endothelial cells. Nature 1988;332:411–415. [PubMed: 2451132]

Zhao H, Sapolsky RM, Steinberg GK. Interrupting reperfusion as a stroke therapy: ischemic postconditioning reduces infarct size after focal ischemia in rats. J Cereb Blood Flow Metab 2006;26:1114–1121. [PubMed: 16736038]

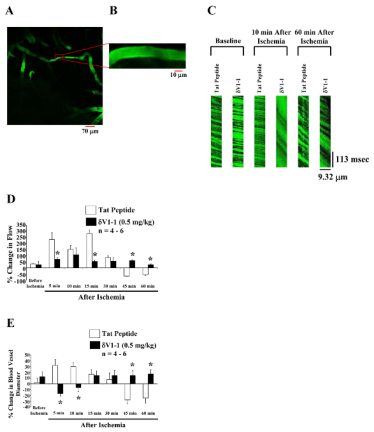

Figure 1.

In vivo imaging of cerebral blood vessels using 2-photon microscopy. Rats were injected with fluorescein isothiocyanate (FITC)-dextran (0.2 mg/kg) shown in green (**A** and **B**). Images were captured at 20 X (**A**) and 200 X (**B**) of a particular cortical blood vessel. Blood flow measurement using linescans of single vessels (linescans at 512 Hz were used to determine RBC flow) (**C**). RBC flow values were calculated based on the slope of the shadows (measured using NIH Image J) produced by RBCs when traversed through the blood vessel. The slope of each shadow was calculated, averaged, and expressed as percent change in flow over time before and up to 60 min after ischemia (via 2-VO) pretreated with δV1-1 or tat peptide (vehicle) (**D**). Rats pretreated (30 min) with δV1-1 induced attenuation of hyperemia resulting in a decrease in CBF 5 and 15 min after 2-VO, while attenuating hypoperfusion by enhancing CBF 45 and 60 min after ischemia. Cerebral microvessel diameters are measured by capturing images similar to Figure 1B (**E**). Rats pretreated (30 min) with δV1-1 reversed post-ischemic hyperemia and hypoperfusion suggesting vasoconstriction (decreased blood vessel diameter, 5 and 10 min after ischemia.) followed by vasodilation (increased blood vessel diameter, 45 and 60 min after ischemia) of cortical microvessels (n = 4 – 6). * indicates $p \leq 0.05$ as compared to tat peptide at the respective time point.

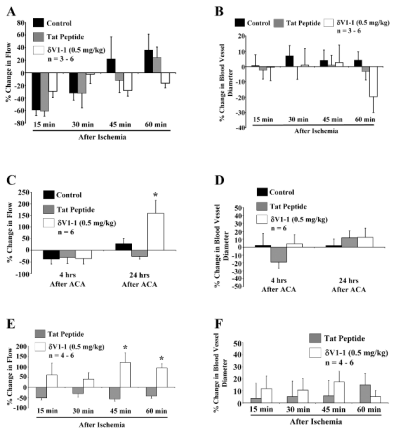

Figure 2.

δV1-1-induced attenuation of hypoperfusion 24 hrs after ACA. Similar experimental profile was used as described in Figure 1. 2-PM was used to image rat cortical microvessels before and after 6 min of ACA pretreated with tat peptide or δV1-1. Rats pretreated with tat peptide or δV1-1 was subjected to 6 min of ACA. 2-PM imaging analysis of cortical microvessels was performed before and after ACA (15 – 60 min) resulting in no significant change in overall cortical blood flow (**A**) or blood vessel diameter (**B**) (n = 3 – 6). Rats pretreated (30 min) with δV1-1 after 24 hrs of ACA significantly enhanced cortical microvessel blood flow by 160 % (C) with no change in blood vessel diameters detected 4 or 24 hrs after ACA in the presence or absence of δV1-1 (D) (n = 6). In a separate set of experiments, δV1-1 was administered directly after 6 min of ACA and CBF changes were monitored. CBF was enhanced 45 and 60 min after ACA (**E**), but no significant changes in blood vessel diameters were detected (n = 4 – 6) (**F**). * indicates $p \leq 0.05$ as compared to tat peptide at the respective time point.

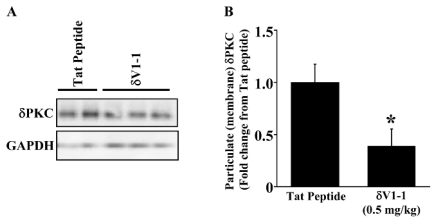

Figure 3.

δV1-1 inhibits δPKC translocation in cortical lysates. 24 hours after ACA, the animals were sacrificed and the cortex (site of 2-PM observed CBF) was extracted for Western blot analyses. Pretreatment with δV1-1 in the rat inhibited δPKC translocation after 6 min of ACA (A) with a 61 % reduction as compared to tat peptide (vehicle) treatment summarized in (**B**) (n = 4 – 6). Glyceraldehyde 3-phosphate dehydrogenase (GAPDH) was used as a loading control in all samples. * indicates $p \leq 0.05$ as compared to tat peptide.

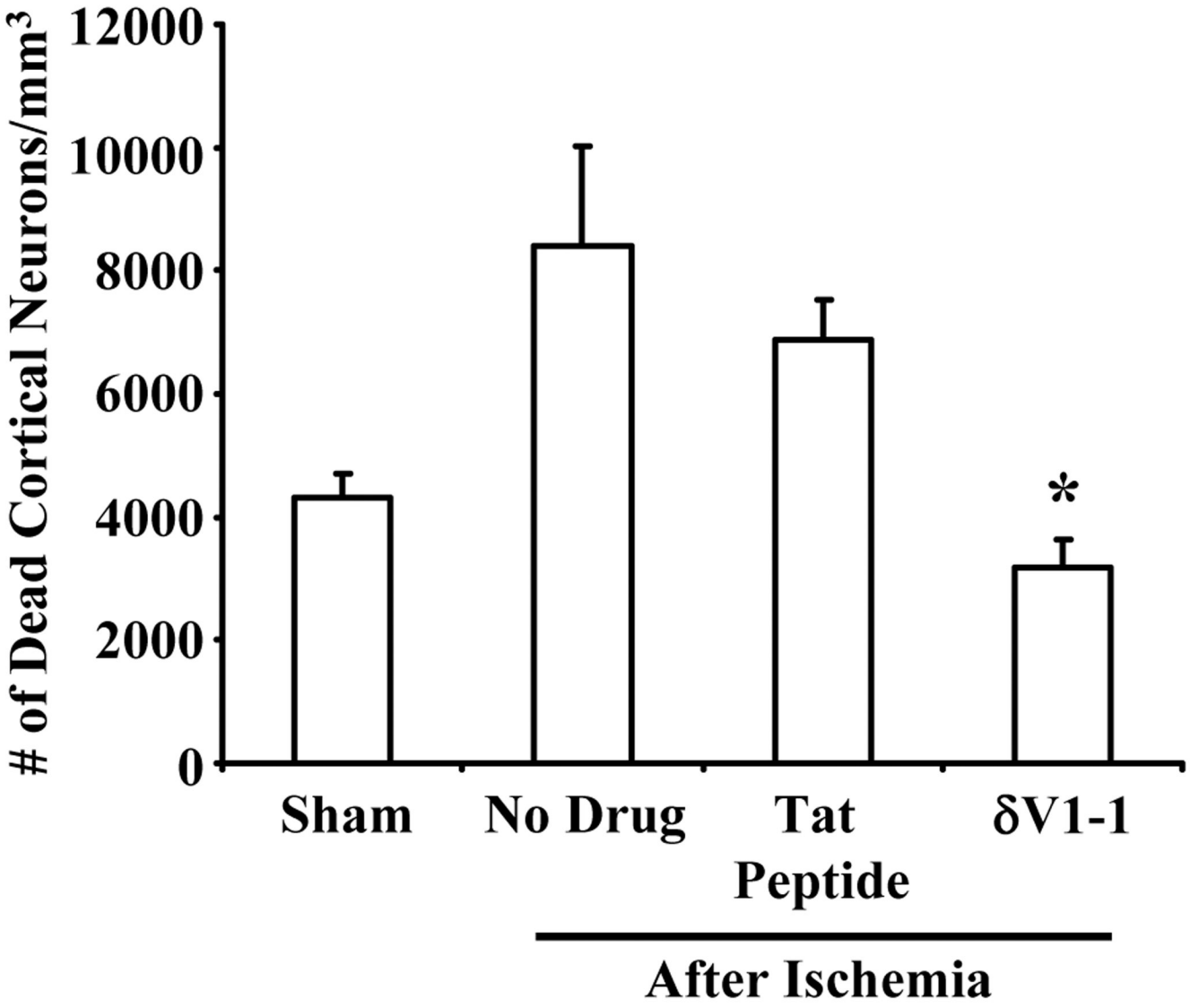

Figure 4.

δV1-1 provides neuroprotection in the cortex regions 7 days after ACA. Rats pretreated with δV1-1 or tat peptide were subjected to 6 min of ACA. Since cortical CBF was measured throughout this study (via 2-PM method), we determined the number of dead cortical neurons in the same region as CBF measurements. Rats pretreated with δV1-1 presented with lower number of dead cortical neurons as compared to no drug and tat peptide experimental groups after ACA ($n = 3 – 11$, * $p \leq 0.05$).

Neuroscience. Author manuscript; available in PMC 2011 December 1.

Table 1

Asphyxial Cardiac Arrest Physiological Parameters

Group	Variable	Before ACA	After ACA	4hrs after ACA	24hrs after ACA
ACA	**Body wt (g)**	322.5 ± 2.9	–	–	–
(n = 6)	**pH**	7.452 ± 0.018	7.309 ± 0.023*	7.436 ± 0.021	7.406 ± 0.00412
	PCO_2 (mm Hg)	39.0 ± 1.4	40.1 ± 2.7	32.9 ± 0.99	37.9 ± 2.7
	PO_2 (mm Hg)	127.9 ± 8.3	361 ± 52*	195 ± 36	133.3 ± 8.3
	MABP (mm Hg)	133.7 ± 3.2	114.1 ± 4.7	111.8 ± 5.1	117.1 ± 7.8
	Blood				
	glucose (mg/dL)	144 ± 10	–	–	–
Tat+ACA	**Body wt (g)**	334 ± 12	–	–	–
(n = 6)	**pH**	7.438 ± 0.012	7.321 ± 0.033*	7.442 ± 0.032	7.449 ± 0.019
	PCO_2 (mm Hg)	38.3 ± 1.9	35.5 ± 1.7	38.0 ± 4.8	36.7 ± 1.9
	PO_2 (mm Hg)	116 ± 12	277 ± 48*	157 ± 37	138 ± 10
	MABP (mm Hg)	127 ± 10	113.8 ± 6.2	99 ± 14	104.3 ± 5.6
	Blood				
	glucose (mg/dL)	125 ± 12	–	–	–
δV1-1 +	**Body wt (g)**	335 ± 15	–	–	–
ACA	**pH**	7.454 ± 0.016	7.343 ± 0.044*	7.503 ± 0.024	7.449 ± 0.015
(n = 6)	**PCO_2 (mm Hg)**	37.9 ± 1.0	38.0 ± 3.4	31.9 ± 2.2	34.1 ± 1.3
	PO_2 (mm Hg)	128.4 ± 8.8	261 ± 53*	175 ± 47	134 ± 13
	MABP (mm Hg)	111.5 ± 4.9	100.0 ± 2.8	107.0 ± 8.1	110.3 ± 6.4
	Blood				
	glucose (mg/dL)	128 ± 14	–	–	–

*indicates significant difference from baseline (Before ACA). We observed the animal to possess slight acidosis shortly after ACA, but was normalized 4 and 24 hrs after ACA. Partial pressure of oxygen (PO_2) for all groups (After ACA) were greater than 150 mmHg, due to 100 % delivery of oxygen and increased ventilator rate (60 breaths/min to 80 breaths/min) during and after resuscitation.

Table 2

Physiological Parameters from Western Blot Analysis

Group	Variable	Before ACA	After ACA
Tat+ACA	**Body wt (g)**	288 ± 15	–
(n = 4)	**pH**	7.4433 ± 0.0088	7.4390 ± 0.0095
	PCO_2 (mm Hg)	34.67 ± 0.33	32.0 ± 1.0
	PO_2 (mm Hg)	115.7 ± 9.9	386.3 ± 65.9*
	MABP (mm Hg)	115.7 ± 0.67	103.3 ± 3.3
	Blood		
	glucose (mg/dL)	116.3 ± 7.6	–
δV1-1 +	**Body wt (g)**	314.8 ± 6.6	–
ACA	**pH**	7.429 ± 0.013	7.465 ± 0.030
(n = 6)	**PCO_2 (mm Hg)**	37.9 ± 1.2	35.8 ± 2.1
	PO_2 (mm Hg)	134.9 ± 8.9	412 ± 56*
	MABP (mm Hg)	111.8 ± 5.1	104.5 ± 4.0
	Blood		
	glucose (mg/dL)	106 ± 12	–

* indicates significant difference from baseline (Before ACA). PO_2 for all groups (After ACA) were greater than 150 mmHg, due to 100 % delivery of oxygen and increased ventilator rate (60 breaths/min to 80 breaths/min) during and after resuscitation.

Table 3

Histopathology Physiological Parameters

Group	Variable	Before ACA	After ACA
Sham	**Body wt (g)**	284.1 ± 2.4	–
(n = 8)	**pH**	7.455 ± 0.012	7.432 ± 0.018
	PCO_2 (mm Hg)	37.30 ± 0.58	38.00 ± 0.82
	PO_2 (mm Hg)	164.4 ± 7.5	148.6 ± 9.2
	MABP (mm Hg)	117.4 ± 2.5	119.8 ± 3.8
	Blood		
	glucose (mg/dL)	165 ± 10	–
ACA	**Body wt (g)**	320.6 ± 15	–
(n = 3)	**pH**	7.446 ± 0.013	7.371 ± 0.019*
	PCO_2 (mm Hg)	38.18 ± 0.90	39.79 ± 0.94
	PO_2 (mm Hg)	133.8 ± 7.5	334 ± 87*
	MABP (mm Hg)	113.1 ± 7.8	106.9 ± 8.8
	Blood		
	glucose (mg/dL)	184 ± 25	–
Tat+	**Body wt (g)**	302.7 ± 6.9	–
ACA	**pH**	7.4676 ± 0.0089	7.421 ± 0.018*
(n = 11)	**PCO_2 (mm Hg)**	36.9 ± 0.95	36.10 ± 0.74
	PO_2 (mm Hg)	148.0 ± 8.6	354 ± 41*
	MABP (mm Hg)	121.7 ± 4.6	116.7 ± 4.6
	Blood		
	glucose (mg/dL)	175.3 ± 6.1	–
δV1-1+	**Body wt (g)**	324.6 ± 7.8	–
ACA	**pH**	7.4354 ± 0.0095	7.404 ± 0.013
(n = 9)	**PCO_2 (mm Hg)**	38.93 ± 0.93	40.0 ± 1.3
	PO_2 (mm Hg)	148.4 ± 9.8	430 ± 28*
	MABP (mm Hg)	114.6 ± 4.6	118.3 ± 5.4
	Blood		
	glucose (mg/dL)	197 ± 12	–

* indicates significant difference from baseline (Before ACA). We observed that some animals possess slight acidosis shortly after ACA. PO_2 for all groups (with the exception of sham) were greater than 148 mmHg, due to 100 % delivery of oxygen and increased ventilator rate (60 breaths/min to 80 breaths/min) during and after resuscitation.